QCD corrections to longitudinal spin asymmetries in W±-boson production at RHIC

von Arx, C ; Gehrmann, T

Abstract: The polarized antiquark distributions in the proton can be measured by studying spin asymmetries in vector boson production in longitudinally polarized proton–proton collisions. The STAR and PHENIX experiments at BNL RHIC have reported first observations of single spin asymmetries in W± production most recently. We compute the QCD corrections to single and double spin asymmetries, taking account of the leptonic decay of the W± boson and of restrictions on the kinematical acceptance of the detectors. The QCD corrections have only a small impact on the asymmetries, such that a reliable extraction of the polarized antiquark distributions can be envisaged once more precise measurements are made.

DOI: https://doi.org/10.1016/j.physletb.2011.04.062

Originally published at:
von Arx, C; Gehrmann, T (2011). QCD corrections to longitudinal spin asymmetries in W±-boson production at RHIC. Physics Letters B, 700(1):49-54.
DOI: https://doi.org/10.1016/j.physletb.2011.04.062

ZU-TH 03/11

QCD corrections to longitudinal spin asymmetries in $W^{\pm}$-boson production at RHIC

C. von Arx[a, *] and T. Gehrmann[b]

[a] *Departement Physik, Universität Basel, Klingelbergstrasse 82, CH-4056 Basel, Switzerland*

[b] *Institut für Theoretische Physik, Universität Zürich, Winterthurerstrasse 190, CH-8057 Zürich, Switzerland*

Abstract

The polarized antiquark distributions in the proton can be measured by studying spin asymmetries in vector boson production in longitudinally polarized proton-proton collisions. The STAR and PHENIX experiments at BNL RHIC have reported first observations of single spin asymmetries in $W^{\pm}$-production most recently. We compute the QCD corrections to single and double spin asymmetries, taking account of the leptonic decay of the $W^{\pm}$ boson and of restrictions on the kinematical acceptance of the detectors. The QCD corrections have only a small impact on the asymmetries, such that a reliable extraction of the polarized antiquark distributions can be envisaged once more precise measurements are made.

[*] present address: Swiss Federal Nuclear Safety Inspectorate, CH-5200 Brugg

1 Introduction

Owing to a large variety of measurements, the unpolarized parton distributions are known to high precision [1–5]. Determinations of the polarized parton distributions [6, 7] have to rely on a much smaller data set, consisting mainly of inclusive and semi-inclusive polarized deep inelastic scattering measurements on fixed targets, augmented with single inclusive hadron and jet measurements from RHIC. As a result, the polarized quark distributions in the proton are determined accurately, while constraints on the polarized antiquark and gluon distributions are much less stringent. Semi-inclusive polarized deep inelastic scattering provides some information on the antiquark distributions of different flavors, although this extraction is not free from ambiguities, since it requires the quark-to-hadron fragmentation functions as input.

A very clean measurement of the polarized antiquark distributions in the proton can be made from spin asymmetries in electroweak vector boson production in polarized proton-proton collisions [8]. Owing to the parity-violating coupling of the $W^{\pm}$ and Z^0 bosons, non-vanishing spin asymmetries are already obtained in the collision of one polarized and one unpolarized proton (single spin asymmetries), in addition to the more common double spin asymmetries. Measurements of these asymmetries are possible at the BNL RHIC collider, and both the STAR and PHENIX experiments have recently reported a first observation of single spin asymmetries in $W^{\pm}$ production [9,10]. At present, these data are not yet sufficiently precise (and do not cover a large enough kinematical range) to provide competitive constraints on the polarized antiquark distributions. However, future polarized proton runs at RHIC will improve upon this situation and are likely to yield precision measurements of the spin asymmetries in $W^{\pm}$ production.

To include these data in global fits of polarized parton distributions at next-to-leading order (NLO), the NLO QCD corrections must be taken into account in the evaluation of the asymmetries. These corrections are known already for a long time for the fully inclusive asymmetries in gauge boson production [11, 12] and for the asymmetries differential in the gauge boson rapidity [13, 14]. Since $W^{\pm}$-boson production is observed only through the decay into a lepton and a neutrino, the $W^{\pm}$-boson rapidity cannot be measured directly. By accurately determining the missing transverse momentum due to the unobserved neutrino and measuring the lepton transverse momentum and rapidity, the $W^{\pm}$-boson rapidity can in principle be inferred from kinematical constraints. With the limited coverage of the STAR and PHENIX detectors, such a determination is however not possible. Instead, one measures the asymmetries as a function of the kinematics of the observed final-state lepton: lepton rapidity y_l and lepton transverse momentum $p_{T,l}$. These correlate closely with the $W^{\pm}$-boson rapidity, but the interpretation of the resulting asymmetries in terms of the polarized parton distributions is less straightforward.

It is the aim of this paper to derive the NLO QCD corrections to the single and double spin asymmetries in $W^{\pm}$ production as function of the observed lepton rapidity and transverse momentum. For the single spin asymmetries, these corrections were recently obtained by de Florian and Vogelsang in [15], and our calculation provides an independent validation of their results. Higher-order QCD effects in the asymmetries, including resummation of large logarithmic corrections, were studied previously in [16] and are implemented in the widely used RHICBOS program.

This paper is structured as follows: in Section 2, we introduce the single and double spin asymmetries in $W^{\pm}$-boson production and discuss their interpretation in terms of polarized parton distributions. Section 3 briefly reviews the technical aspects of the NLO calculation, while Section 4 discusses the numerical impact of the NLO corrections. We compare the NLO results to the recent STAR and PHENIX measurements in Section 5 and conclude with Section 6.

2 Single and double spin asymmetries in vector boson production

The single and double spin asymmetries in vector boson production processes are constructed from the helicity-dependent production cross sections

$$\mathrm{d}\sigma^{h_1 h_2}$$

where $h_{1,2} = (+,-)$ denote the helicities of the two incoming hadrons. The coordinate frame is defined such that hadron 1 moves in positive rapidity direction.

The unpolarized cross section is the average over all initial state helicities:

$$\mathrm{d}\sigma = \frac{1}{4}\left(\mathrm{d}\sigma^{++} + \mathrm{d}\sigma^{+-} + \mathrm{d}\sigma^{-+} + \mathrm{d}\sigma^{--}\right) \,, \tag{1}$$

while the singly (only hadron 1 polarized) and doubly polarized cross sections are given by:

$$\mathrm{d}\Delta\sigma_L = \frac{1}{4}\left(\mathrm{d}\sigma^{++} + \mathrm{d}\sigma^{+-} - \mathrm{d}\sigma^{-+} - \mathrm{d}\sigma^{--}\right) \,, \tag{2}$$

$$\mathrm{d}\Delta\sigma_{LL} = \frac{1}{4}\left(\mathrm{d}\sigma^{++} - \mathrm{d}\sigma^{+-} - \mathrm{d}\sigma^{-+} + \mathrm{d}\sigma^{--}\right) \,. \tag{3}$$

From these, single and double spin asymmetries are constructed as functions of kinematical variables of the observed final-state particles. Previous studies on NLO corrections to spin asymmetries in vector boson production [14] focused on the rapidity of the vector boson y, which is itself not directly measurable in $W^{\pm}$ production, due to the unobserved neutrino in the final state.

For the partonic interpretation of the asymmetries, the vector boson rapidity is very instructive, since at leading order (LO) it is directly related to the momentum fractions of the partons probed in both hadrons:

$$x^0_{1,2} = \sqrt{M_W^2/S}\, e^{\pm y}.$$

Restricting to only up and down quarks, one thus finds very simple leading-order expressions for the asymmetries:

$$\begin{aligned}
A_L^{W^+}(y) &= \frac{-\Delta u(x_1^0)\bar{d}(x_2^0) + \Delta\bar{d}(x_1^0)u(x_2^0)}{u(x_1^0)\bar{d}(x_2^0) + \bar{d}(x_1^0)u(x_2^0)}\,, \\
A_L^{W^-}(y) &= \frac{-\Delta d(x_1^0)\bar{u}(x_2^0) + \Delta\bar{u}(x_1^0)d(x_2^0)}{d(x_1^0)\bar{u}(x_2^0) + \bar{u}(x_1^0)d(x_2^0)}\,, \qquad (4) \\
A_{LL}^{W^+}(y) &= -\frac{\Delta u(x_1^0)\Delta\bar{d}(x_2^0) + \Delta\bar{d}(x_1^0)\Delta u(x_2^0)}{u(x_1^0)\bar{d}(x_2^0) + \bar{d}(x_1^0)u(x_2^0)}\,, \\
A_{LL}^{W^-}(y) &= -\frac{\Delta d(x_1^0)\Delta\bar{u}(x_2^0) + \Delta\bar{u}(x_1^0)\Delta d(x_2^0)}{d(x_1^0)\bar{u}(x_2^0) + \bar{u}(x_1^0)d(x_2^0)}\,. \qquad (5)
\end{aligned}$$

At RHIC with $\sqrt{S} = 500$ GeV, these asymmetries are thus sensitive on $x_{1,2} \gtrsim 0.05$. At large and positive rapidity y, $(x_1^0 > x_2^0)$, the single spin asymmetries A_L are dominated by the first term in the numerator, since $\Delta q(x_1^0, Q^2) \gg \Delta\bar{q}(x_1^0, Q^2)$ for large x_1^0. The second term in the numerator is dominant for large and negative y, $(x_1^0 < x_2^0)$, since $q(x_2^0, Q^2) \gg \bar{q}(x_2^0, Q^2)$ for large x_2^0. Given that for the x-range probed by RHIC, the polarized quark distributions are substantially larger than the polarized antiquark distributions, and their sum is well constrained from polarized inclusive deep inelastic scattering [6], the double spin asymmetries can be used for a reliable extraction of $\Delta\bar{u}(x)$ and $\Delta\bar{d}(x)$.

With only the decay lepton being observable, the lepton rapidity y_l and transverse momentum $p_{T,l}$ are the more appropriate kinematical variables. Measurements of the transverse mass, as commonly carried out in vector boson production at the Tevatron, are not feasible at RHIC due to the non-hermetic detector coverage, which prevents a reliable reconstruction of the missing transverse momentum carried by the neutrino.

We shall thus focus on the single and double spin asymmetries

$$A_L(y_l) \equiv \frac{\mathrm{d}\Delta\sigma_L/\mathrm{d}y_l}{\mathrm{d}\sigma/\mathrm{d}y_l}, \qquad A_{LL}(y_l) \equiv \frac{\mathrm{d}\Delta\sigma_{LL}/\mathrm{d}y_l}{\mathrm{d}\sigma/\mathrm{d}y_l} \qquad (6)$$

and

$$A_L(p_{T,l}) \equiv \frac{\mathrm{d}\Delta\sigma_L/\mathrm{d}p_{T,l}}{\mathrm{d}\sigma/\mathrm{d}y_{T,l}}, \qquad A_{LL}(p_{T,l}) \equiv \frac{\mathrm{d}\Delta\sigma_{LL}/\mathrm{d}p_{T,l}}{\mathrm{d}\sigma/\mathrm{d}p_{T,l}}\,. \qquad (7)$$

Polarized and unpolarized cross sections in these asymmetries can be expanded in QCD perturbation theory in the strong coupling constant α_s. In these cross sections, the exchanged $W^\pm$ boson is not required to be on-shell, its finite width is taken into account in its propagator.

3 Next-to-leading order corrections

The next-to-leading order expressions for the asymmetries are obtained by including the $\mathcal{O}(\alpha_s)$ corrections in numerator and denominator. The computation of these corrections is a standard task in higher order calculations, carried out in dimensional regularization in $d = 4 - 2\epsilon$ dimensions. It requires to combine the virtual one-loop corrections to the process $q\bar{q}' \to W^\pm \to l^\pm\nu$

with the real radiation contributions $q\bar{q}' \to W^\pm g \to l^\pm \nu g$ and $qg \to W^\pm q' \to l^\pm \nu q'$. The real radiation contributions develop infrared singularities if the final-state gluon becomes soft, or if the final-state parton becomes collinear with one of the incoming partons. These infrared real radiation singularities can be extracted analytically. They cancel in the final expression for the cross section when combined with the infrared-divergent virtual contributions and with mass factorization counterterms for the incoming parton distributions. Various techniques for the treatment of infrared singular real radiation exist at NLO, based either on introducing subtraction terms [17–19] or on a slicing of the final-state phase space [20, 21].

In our calculation, we use the phase space slicing method [20, 21] for the real radiation contributions. In this method, the real radiation phase space is split into resolved and unresolved regions by introducing a cut-off parameter $s_{\min}$ on all Mandelstam invariants. The resolved regions are integrated numerically, while the unresolved regions are integrated analytically, giving rise to the infrared divergent terms. The phase space slicing contributions from the unresolved regions are universal and depend only on the type of partons involved in the unresolved configuration [20]. These are computed first in a hypothetical kinematical situation with all partons in the final state, and then continued to the true kinematical situation by using a crossing function [21] for each initial state parton. The polarized crossing functions are obtained from the unpolarized expressions in [21] by substituting the d-dimensional unpolarized one-loop splitting functions by their polarized counterparts [22, 23].

Our calculation was validated by comparing the NLO unpolarized differential cross sections $\mathrm{d}\sigma$ against MCFM [24] and the singly polarized differential cross sections $\mathrm{d}\Delta\sigma_L$ against CHE [15] (using the same set of parameters and setting renormalization and factorization scales $\mu^2 = M_W^2$ for the total cross sections and $\mu^2 = (M_W^2 + p_{T,l}^2)/4$ for the distributions, as in [15]). Full agreement is found for both quantities, thereby providing a crucial independent cross-check of [15].

4 Numerical results

Polarized proton-proton collisions are studied at RHIC at different centre-of-mass energies. For vector boson production, only the high-energy runs at $\sqrt{S} = 500$ GeV are of relevance, such that we use this setup for our studies. For the unpolarized parton distribution functions, we use the MRST2002 NLO set [25]; polarized parton distributions are taken from DSSV [6]. The DSSV set is the result of a global fit to spin asymmetries in inclusive and semi-inclusive deep inelastic scattering as well as single inclusive hadron and jet production at RHIC. In its extraction, the unpolarized cross sections entering the asymmetries are computed from the MRST2002 NLO set, such that the DSSV spin-dependent parton distributions should be used consistently with this set. Likewise, the value of the strong coupling constant should be consistent with what is used in the parton distributions, such that we take $\alpha_s(M_Z) = 0.1195$ [25]. Renormalization and factorization scales are taken to be equal, and are fixed to $\mu_R = \mu_F = M_W$. The NLO scale dependence of the single and double spin asymmetries $A_L(y)$ and $A_{LL}(y)$ was studied in detail in [14]. It turns out to be very small, largely due to cancelations between the polarized and

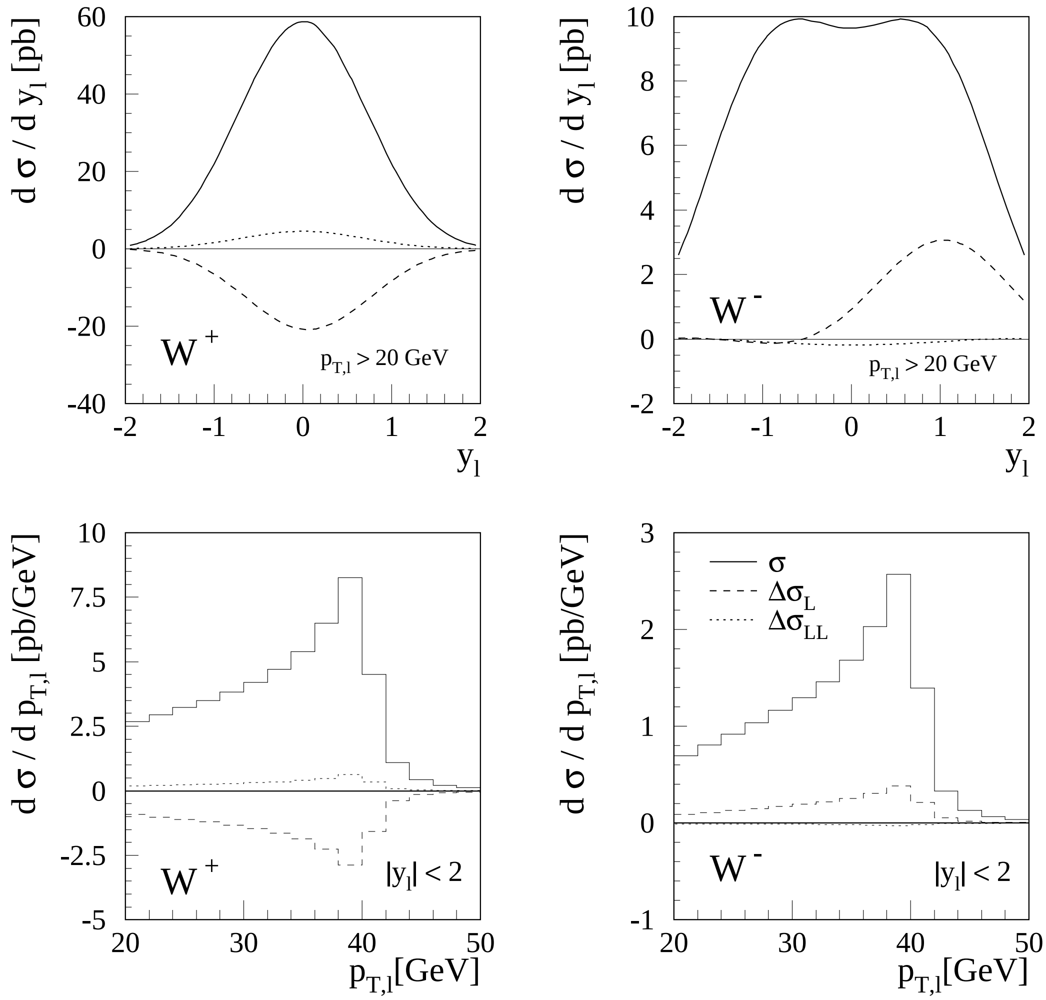

Figure 1: Next-to-leading order differential cross sections for single inclusive lepton production at RHIC, $\sqrt{S} = 500$ GeV with $p_{T,l} > 20$ GeV and $|y_l| < 2$. Solid: unpolarized cross section, dashed: singly polarized, dotted: doubly polarized.

unpolarized cross sections in the asymmetry.

The $W^{\pm}$ mass and width are taken [26] as $M_W = 80.399$ GeV and $\Gamma_W = 2.085$ GeV, and the Fermi coupling as $G_F = 1.16637 \cdot 10^{-5}$ GeV^{-2}. By using the Fermi coupling constant as input parameter, electroweak corrections to the cross sections are minimized. Neglecting incoming bottom quarks, we use the CKM matrix elements $|V_{ud}| = |V_{cs}| = 0.975$ and $|V_{us}| = |V_{cd}| = 0.222$.

As default for our numerical studies, we use the following cuts on the final-state lepton: $p_{T,l} > 20$ GeV and $|\eta_l| < 2$. The unpolarized and polarized NLO cross sections with these cuts are displayed in Figure 1 as function of either y_l or $p_{T,l}$. From these results, it can be anticipated

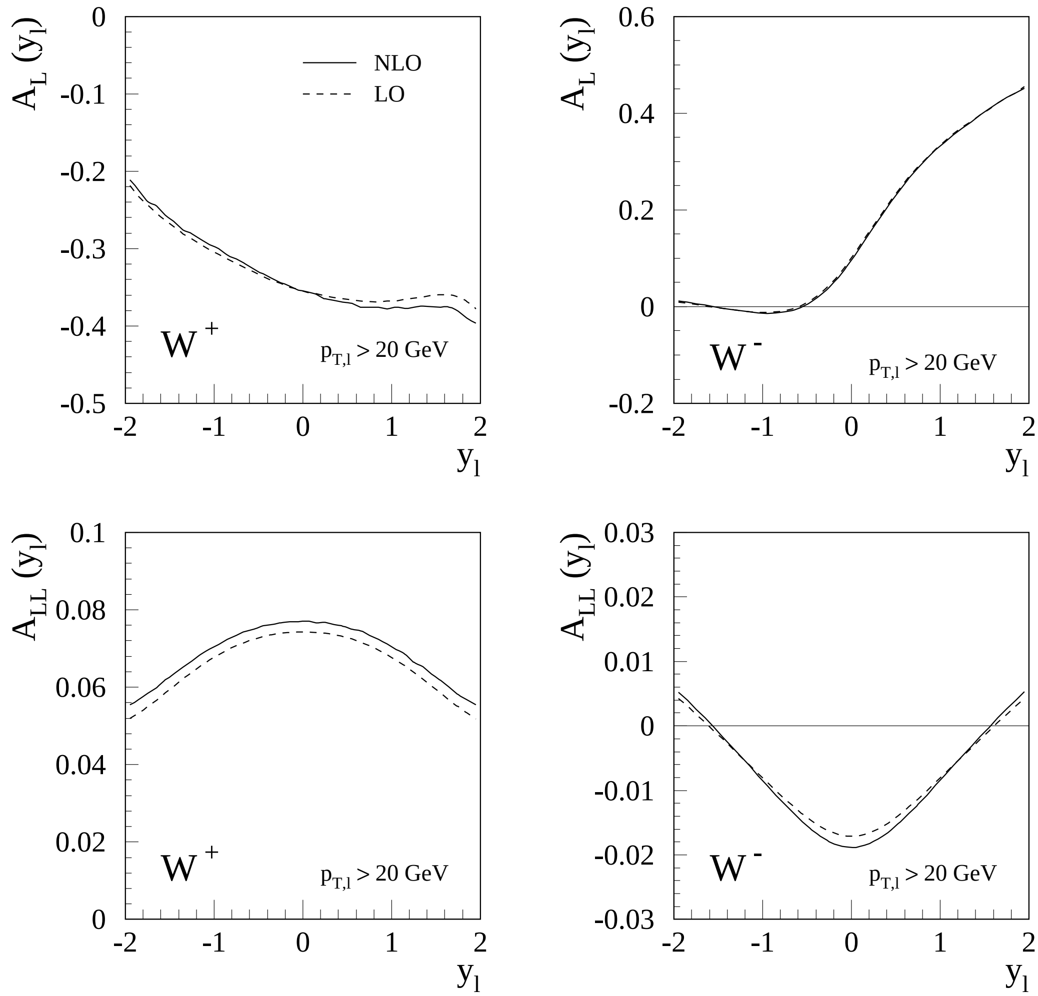

Figure 2: Single and double spin asymmetries as function of y_l at NLO (solid) and LO (dashed).

that the single spin asymmetries are substantially larger than the double spin asymmetries. The transverse momentum distribution of the lepton shows the characteristic peak at $M_W/2$ in the unpolarized and polarized cases. To study the behavior of the polarized cross sections in more detail, the single and double spin asymmetries A_L and A_{LL} are more suitable than the cross sections themselves.

Figures 2 and 3 show these asymmetries as function of y_l and $p_{T,l}$. In these figures, the LO asymmetry is obtained by evaluating polarized and unpolarized cross sections to LO, while both cross sections are evaluated to NLO for the NLO asymmetry. Since this figure aims to quantify the effect of the parton-level NLO corrections, both LO and NLO asymmetry are

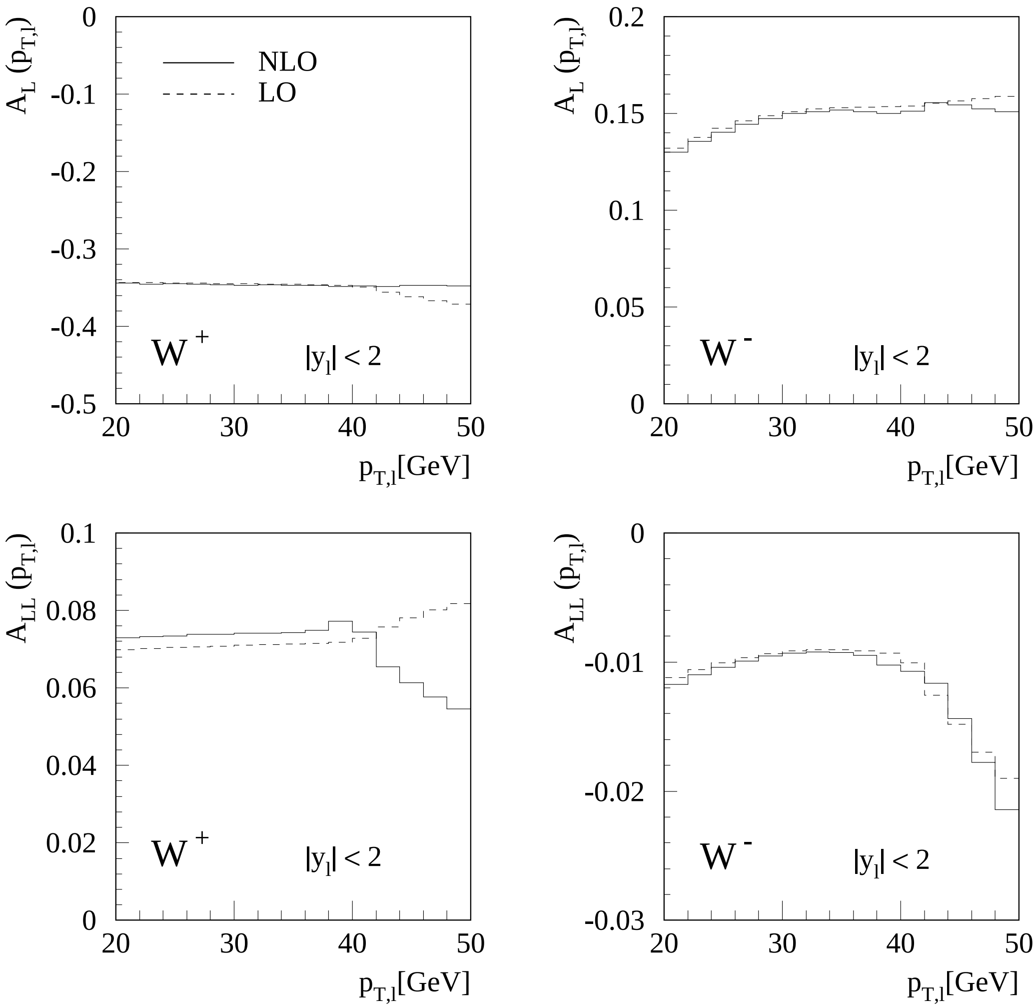

Figure 3: Single and double spin asymmetries as function of $p_{T,l}$ at NLO (solid) and LO (dashed).

evaluated with the same NLO sets of parton distributions. We observe that $A_L(y_l)$ and $A_{LL}(y_l)$ are only very mildly affected by the NLO corrections, and that the corrections do not change the shape of these asymmetries. The corrections to $A_L(p_{T,l})$ and $A_{LL}(p_{T,l})$ are also very small and uniform for $p_{T,l} < M_W/2$, while they become more pronounced for $p_{T,l} > M_W/2$. This behavior can be easily understood from kinematical considerations. At LO, the $W^\pm$ boson is produced at vanishing transverse momentum, such that leptons above $p_{T,l} = M_W/2$ must come from off-shell $W^\pm$ production. The real radiation contributions at NLO lead to final states with a finite transverse momentum of the $W^\pm$, which can thus be near its mass shell. With this new parton-level contribution appearing at NLO, the NLO unpolarized and polarized cross sections

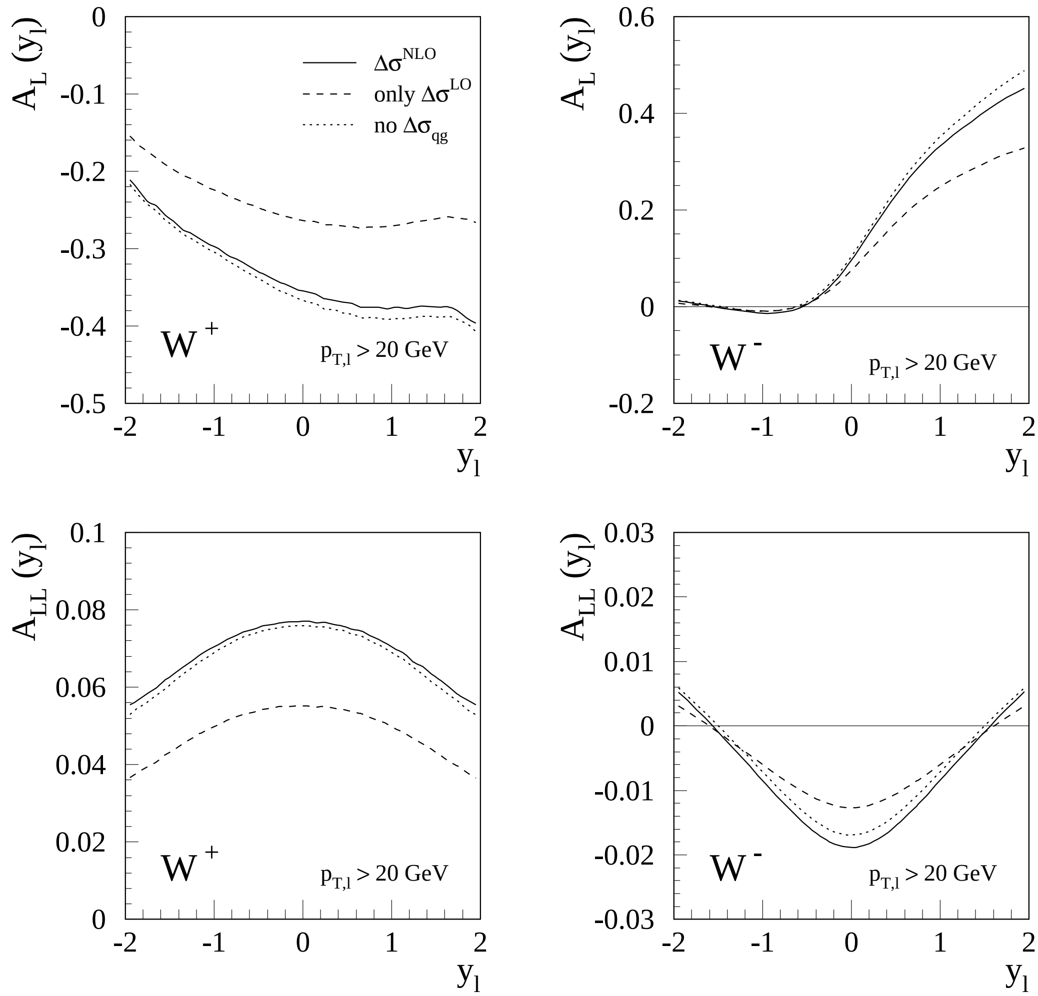

Figure 4: Individual partonic contributions to the single and double spin asymmetries as function of y_l. Unpolarized cross section is always evaluated to NLO, polarized cross section evaluated to NLO (solid), LO (dashed), NLO without qg subprocess (dotted).

for $p_{T,l} > M_W/2$ are much larger than their LO counterparts, and the asymmetry is modified substantially.

Compared to the results of [15], we observe slight discrepancies in $A_L(y_l)$ for large $|y_l|$. These are entirely due to the different choice of renormalization and factorization scales: $\mu^2 = M_W^2$ in our evaluation, compared to $\mu^2 = (M_W^2 + p_{T,l}^2)/4$ in [15]. With the same scale choice (and the same electroweak parameters), we find full agreement with [15].

The numerical importance of the different parton-level contributions to the single and double spin asymmetries is displayed in Figures 2 and 3. All asymmetries in these figures are normal-

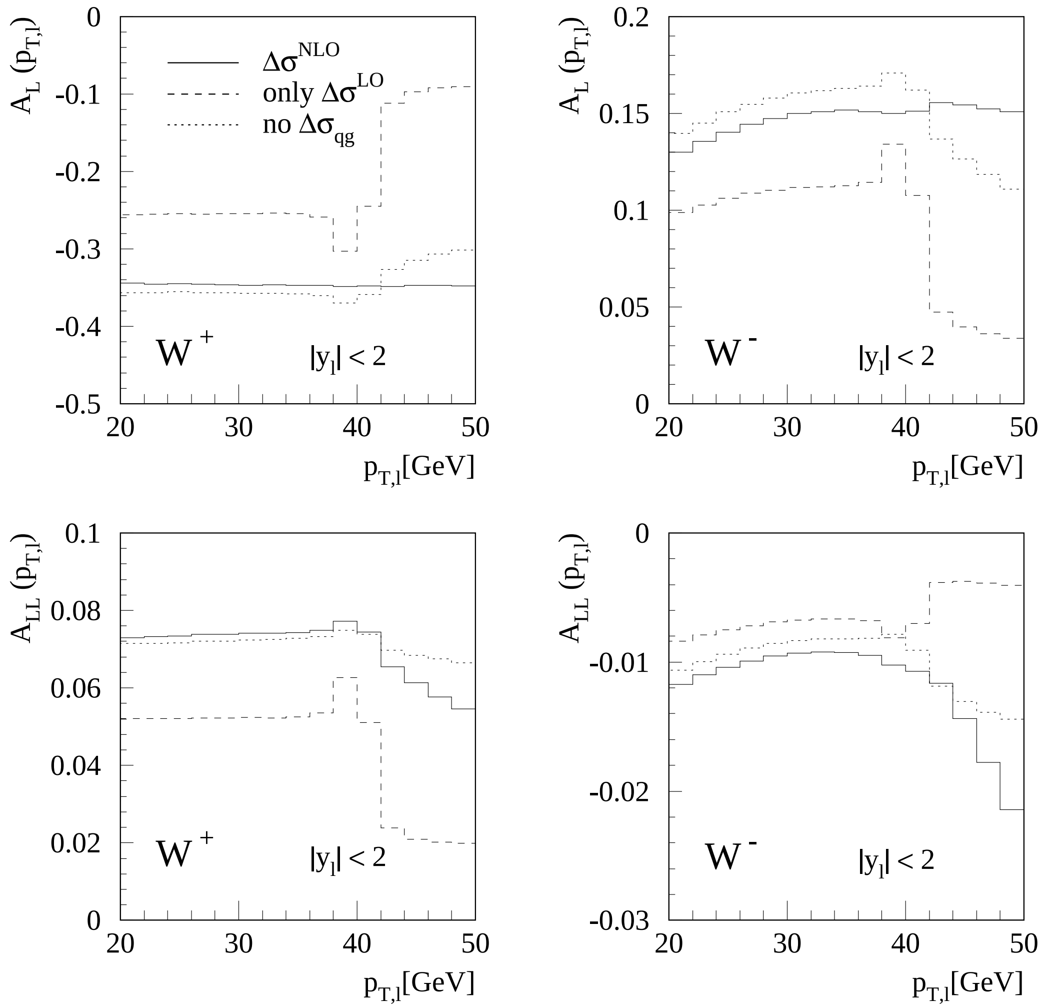

Figure 5: Individual partonic contributions to the single and double spin asymmetries as function of $p_{T,l}$. Unpolarized cross section is always evaluated to NLO, polarized cross section evaluated to NLO (solid), LO (dashed), NLO without qg subprocess (dotted).

ized to the unpolarized cross sections evaluated at NLO. Comparing the results obtained with $\Delta\sigma$ evaluated only at LO with the LO asymmetries in Figures 2 and 3, one concludes that the smallness of the NLO corrections to the asymmetries is due to a cancelation of the NLO corrections to unpolarized and polarized cross sections in the asymmetry. The NLO corrections to the polarized cross sections are moreover dominated by the $q\bar{q}$ subprocess. Consequently, a future extraction of polarized quark distributions from the $A_L(y_l)$ and $A_{LL}(y_l)$ will not be affected by the uncertainty on the polarized gluon distribution.

	Cuts		A_L (exp)	A_L (LO)	A_L (NLO)
STAR	25 GeV $< p_{T,l} <$ 50 GeV;	W^+	$-0.27 \pm 0.10 \pm 0.02$	-0.347	-0.348
	$\lvert y_l \rvert < 1$	W^-	$0.14 \pm 0.19 \pm 0.02$	0.127	0.123
PHENIX	30 GeV $< p_{T,l} <$ 50 GeV;	W^+	$-0.86^{+0.30}_{-0.14}$	-0.342	-0.342
	$\lvert y_l \rvert < 0.35$	W^-	$0.88^{+0.12}_{-0.71}$	0.107	0.103

Table 1: Single spin asymmetries measured in $W^{\pm}$ production at RHIC by STAR [9] and PHENIX [10] compared to LO and NLO QCD predictions.

5 Comparison with RHIC data

The single spin asymmetries A_L in $W^{\pm}$-boson production have been measured recently at RHIC by the STAR [9] and PHENIX [10] experiments. Both measurements are based on detecting only electrons and positrons at large transverse momentum. Cuts are imposed on the lepton transverse momentum and rapidity, and the measurement is performed in a single bin. Especially the PHENIX measurement relies on a very limited kinematical coverage, such that $W^{\pm}$ and Z^0 boson production cannot be disentangled, since the second lepton from the Z^0 decay is often outside the coverage. The Z^0-boson contributions to the single spin asymmetries at NLO were investigated in [15].

In Table 1, we summarize the experimental cuts and compare the experimentally measured asymmetries with the theoretical predictions at LO and NLO. We observe that the predictions for the asymmetries are perturbatively very stable, with practically no shift observed for the W^+ production, and only a modification of four per cent for the W^- production. The asymmetries observed by STAR are in good agreement with the theoretical prediction, while PHENIX typically obtains asymmetries with a larger magnitude than expected, although with large errors. Both measurements have clearly demonstrated the existence of single spin asymmetries in $W^{\pm}$ production, but not yet attained sufficient precision to provide meaningful constraints on the polarized antiquark distributions.

Future more precise data on the single spin asymmetries, as well as first data on the double spin asymmetries will provide very important input to the determination of the polarized parton distributions.

6 Conclusions

Spin asymmetries in gauge boson production in polarized proton-proton collisions are currently measured at RHIC [9, 10]. These asymmetries provide a direct measurement of the polarized light antiquark distributions, which were only loosely constrained from semi-inclusive polarized deep inelastic scattering up to now [6, 7]. In this paper, we derived the NLO QCD corrections to single and double spin asymmetries in $W^{\pm}$ boson production in polarized proton-proton collisions as function of the measurable final-state lepton variables. Our results for the single spin asymmetries confirm a recent calculation of de Florian and Vogelsang [15].

We show that the NLO corrections have only a very moderate impact on the asymmetries, and that the corrections are largely independent on the at present poorly constrained polarized gluon distribution. Their inclusion is nevertheless mandatory in future global NLO fits of polarized parton distributions for the sake of internal perturbative consistency.

Acknowledgements

We would like to thank Daniel de Florian and Werner Vogelsang for help in comparing with the results presented in [15]. This research was supported by the Swiss National Science Foundation (SNF) under contracts 200020-126691 and 200020-122287.

References

[1] A.D. Martin, W.J. Stirling, R.S. Thorne and G. Watt, Eur. Phys. J. C **63** (2009) 189 [0901.0002].

[2] P. Jimenez-Delgado and E. Reya, Phys. Rev. D **79** (2009) 074023 [0810.4274].

[3] S. Alekhin, J. Blümlein, S. Klein and S. Moch, Phys. Rev. D **81** (2010) 014032 [0908.2766].

[4] H.L. Lai, M. Guzzi, J. Huston, Z. Li, P.M. Nadolsky, J. Pumplin and C.P. Yuan, Phys. Rev. D **82** (2010) 074024 [1007.2241].

[5] R.D. Ball, L. Del Debbio, S. Forte, A. Guffanti, J.I. Latorre, J. Rojo and M. Ubiali, Nucl. Phys. B **838** (2010) 136 [1002.4407].

[6] D. de Florian, R. Sassot, M. Stratmann and W. Vogelsang, Phys. Rev. D **80** (2009) 034030 [0904.3821].

[7] T. Gehrmann and W. J. Stirling, Phys. Rev. D **53** (1996) 6100 [hep-ph/9512406];
D. de Florian, G.A. Navarro and R. Sassot, Phys. Rev. D **71** (2005) 094018 [hep-ph/0504155];
E. Leader, A.V. Sidorov and D.B. Stamenov, Phys. Rev. D **75** (2007) 074027 [hep-ph/0612360];
M. Hirai and S. Kumano [Asymmetry Analysis Collaboration], Nucl. Phys. B **813** (2009) 106 [0808.0413];
J. Blümlein and H. Böttcher, Nucl. Phys. B **841** (2010) 205 [1005.3113].

[8] E. Leader and K. Sridhar, Phys. Lett. B **311** (1993) 324;
C. Bourrely and J. Soffer, Phys. Lett. B **314** (1993) 132; Nucl. Phys. B **423** (1994) 329 [hep-ph/9405250].

[9] M.M. Aggarwal *et al.* [STAR Collaboration], Phys. Rev. Lett. **106** (2011) 062002 [1009.0326].

[10] A. Adare *et al.* [PHENIX Collaboration], Phys. Rev. Lett. **106** (2011) 062001 [1009.0505].

[11] P. Ratcliffe, Nucl. Phys. B **223** (1983) 45.

[12] A. Weber, Nucl. Phys. B **382** (1992) 63;
A. Weber, Nucl. Phys. B **403** (1993) 545;
B. Kamal, Phys. Rev. D **53** (1996) 1142 [hep-ph/9511217].

[13] T. Gehrmann, Nucl. Phys. B **498** (1997) 245 [hep-ph/9702263].

[14] T. Gehrmann, Nucl. Phys. B **534** (1998) 21 [hep-ph/9710508].

[15] D. de Florian and W. Vogelsang, Phys. Rev. D **81** (2010) 094020 [1003.4533].

[16] P.M. Nadolsky and C. P. Yuan, Nucl. Phys. B **666** (2003) 3 [hep-ph/0304001]; **666** (2003) 31 [hep-ph/0304002].

[17] S. Catani and M.H. Seymour, Nucl. Phys. B **485** (1997) 291 [hep-ph/9605323].

[18] S. Frixione, Z. Kunszt and A. Signer, Nucl. Phys. B **467**, 399 (1996) [hep-ph/9512328].

[19] D.A. Kosower, Phys. Rev. D **57** (1998) 5410 [hep-ph/9710213]; **71** (2005) 045016 [hep-ph/0311272];
A. Daleo, T. Gehrmann and D. Maître, JHEP **0704** (2007) 016 [hep-ph/0612257].

[20] W.T. Giele and E.W.N. Glover, Phys. Rev. D **46** (1992) 1980.

[21] W.T. Giele, E.W.N. Glover and D.A. Kosower, Nucl. Phys. B **403** (1993) 633 [hep-ph/9302225].

[22] R. Mertig and W.L. van Neerven, Z. Phys. C **70** (1996) 637 [hep-ph/9506451].

[23] W. Vogelsang, Phys. Rev. D **54** (1996) 2023 [hep-ph/9512218].

[24] J.M. Campbell and R.K. Ellis, Phys. Rev. D **60** (1999) 113006 [hep-ph/9905386].

[25] A.D. Martin, R.G. Roberts, W.J. Stirling and R.S. Thorne, Eur. Phys. J. C **28** (2003) 455 [hep-ph/0211080].

[26] K. Nakamura *et al.* [Particle Data Group], J. Phys. G **37** (2010) 075021.